https://doi.org/10.20965/jaciii.2010.p0714

Paper:

FPGA-Based Relative Distance Estimation for Indoor Robot Control Using Monocular Digital Camera

Ying-Hao Yu*, Chau Vo-Ky, Sarath Kodagoda*, and Quang Phuc Ha***

*School of Electrical, Mechanical and Mechatronic Systems, University of Technology Sydney
PO Box 123, Broadway, NSW 2007, Australia
E-mail: {YingHao.Yu, Sarath.Kodagoda, quangha}@eng.uts.edu.au
**Faculty of Electrical and Electronics Engineering, HoChiMinh University of Technology
268 Ly Thuong Kiet St., Distr. 10, HoChiMinh City, Vietnam
E-mail: chauvoky@gmail.com
[Received February 10, 2010; accepted April 10, 2010]

Distance measurement methodologies based on the digital camera usually require time-consuming calibration procedures, some are even derived from complicated image processing algorithms resulting in low picture frame rates. In a dynamic camera system, due to the unpredictability of intrinsic and extrinsic parameters, odometric results are highly dependent on the quality of extra sensors. In this paper, a simple and efficient algorithm is proposed for relative distance estimation in robotic active vision by using a monocular digital camera. Accuracy of the estimation is achieved by judging the 2D perspective projection image ratio of the robot labels obtained on a TFT-LCD (Thin Film Transistor – Liquid Crystal Display) monitor without the need of any additional sensory cost and complicated calibration effort. Further, the proposed algorithm does not contain any trigonometric functions so that it can be easily implemented on an embedded system using the Field Programmable Gate Array (FPGA) technology. Experimental results are included to demonstrate the effectiveness of the technique.

Keywords: FPGA, relative distance measurement, multi-robot system, perspective projection image

1. Introduction

For relative distance measurement and localization in a multiple robot system, the use of laser range finders [1], ultrasonic sensors [2], or communication networks [3] is quite popular. Laser range finders and ultrasonic sensors use the concept of Time-of-Flight (TOF) to measure the relative distance between two robots. In communication networks, distance measurement requires a routing time and also reception of a Radio Signal Strength Indication (RSSI). The robot will then be able to perform odometry by judging the attenuation of radio strength from adjacent objects [4]. Although these sensors are feasible for range measurement, there are few disadvantages due to the limited information content. For example, they may not be able to comprehensively understand and model the operating environment. In contrast, digital cameras seem to be more versatile owing to a large amount of information in terms of texture, color, illumination, edges, optical flows, distance, etc. Furthermore, while the use of laser, ultrasonic, and radio signals may be limited by active interferences due to crowded sensors, the camera, being a passive sensor, has no such limitation.

Recently, the combination of infrared (or laser) and digital camera sensors is reported as a feasible technology for odometry purposes via Time-of-Flight (TOF) measurement using a camera. It measures the traveling time of the reflected light between the camera and the target. This distance is then presented in a depth map [5]. Unfortunately, these kinds of camera designs usually have disadvantages in a low dynamic range of depth maps, high power consumption for active illumination with LEDs, and computational complexity [6]. Therefore, they are generally not considered in the design of embedded systems in ubiquitous robotics [7] using ambient intelligence whereby limited power capacity remains the first priority.

Despite possible improvements of power capacity with energy saving components and new battery technologies in the future, the real-time computation has become an issue in wireless communication networks [8], where the external server needs to accommodate to computation requirements. This can lead to other problems due to inherent bottlenecks of the network data throughput and security problems. Consequently, in recent years, global camera systems with onboard computation [9] are increasingly popular in distance measurement. For a fixed camera set up, it is possible to determine the distance to an object based on color region [10] and optical properties [11] as:

$$\frac{1}{x}+\frac{1}{y}=\frac{1}{f} \quad \ldots\ldots\ldots\ldots\ldots\ldots (1)$$

$$\frac{h_o}{h'_o}=-\frac{x}{y}, \quad \ldots\ldots\ldots\ldots\ldots\ldots (2)$$

where x is the distance from the object to the camera lens with its perpendicular height h_o, f is the lens focus,

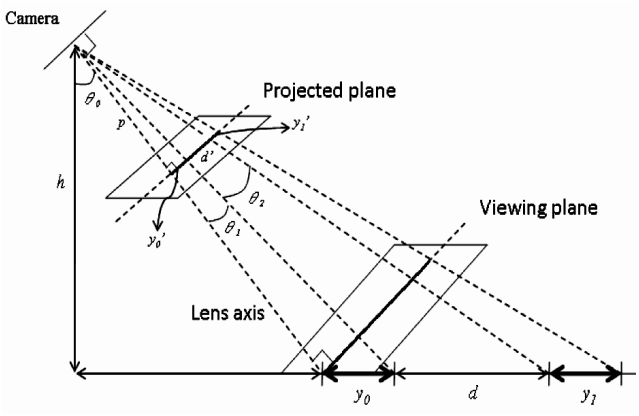

Fig. 1. Image projection in a global camera system with 2D labels in single direction view.

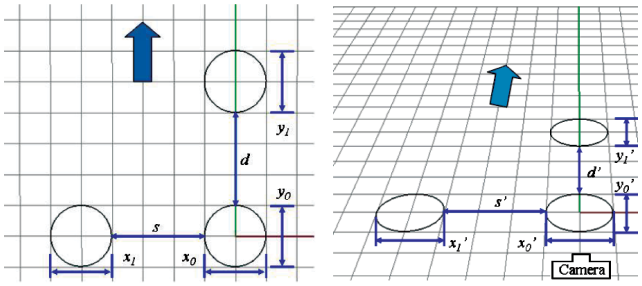

(a) Formation configuration (b) Perspective view

Fig. 2. Deployed robots and their perspective images.

and y is the image distance with relative pixel height h'_o on the camera digital sensor array. In practical applications, Eqs. (1) and (2) can also be modified for real-world applications such as obstacle detection in smart car systems [12]. For this, it is convenient to compare the variant dimension of images by shifting the camera position on a straight line [11].

For indoor robot navigation, the control of multiple robots in a formation often requires a flat floor and available information of relative distances between robots [13]. To localize robots markers are installed on the floor [14] or attached as visual features onto the robots so that they can be easily detected by a global camera system without modifying the indoor environment [15]. However, depending on where the camera is mounted, scene interpretation and depth calculation may involve complicated expressions, as illustrated in **Fig. 1**.

The separation distance between robots therein is obtained by a trigonometric equation:

$$d = h\left[\tan\left(\theta_0 + \tan^{-1}\frac{y'_0 + d'}{p}\right) - \tan\left(\theta_0 + \tan^{-1}\frac{y'_0}{p}\right)\right]. \quad \ldots\ldots (3)$$

Here, h is the installation height of the camera lens, p is the projected image distance from the image sensor array to lens, y_1 and y_0 are the label lengths of leading and following robots, the relative distance between the two robots is d, and the lengths of images on a digital image sensor array are respectively y'_1, d', and y'_0. When the focal length of lens is available, the intrinsic parameters for Eq. (3) can also be decided by a complicated calibration technique [16].

Although the distance given in Eq. (3) is a feasible solution, in a dynamic camera system, the height of camera and its tilting angle θ_0 are usually changing. Furthermore, the focal length of the camera might be unknown, recalibrating camera for every operating instant may be a difficult requirement in real time. Those issues can be overcome by integrating additional sensors and choosing high-end cameras. However, the hardware risk may also occur with all uncertainties of additional sensory readings.

In this paper, we propose a new and efficient relative distance measurement algorithm for monocular cameras, based on the digital photography framework [17]. By detecting the 2D labels on the top of indoor robots, the algorithm can estimate the relative distance between robots by calculating the Perspective Projection Image Ratio (PPIR) of labels, motivated by the usually-adopted human's use of foot length in distance estimation but with a higher accuracy. This algorithm can estimate the relative distance of robots under various dynamic conditions such as unknown tilt angle, height to lens, and focal length of the camera without recalibrating or mounting extra sensors. Moreover, by avoiding all complicated expressions including trigonometric or exponential functions, the algorithm can be implemented in an embedded system using the FPGA technology [18]. Here, unlike [19] where the CORDIC algorithm is used, the PPIR algorithm is based simply on approximating a series.

The paper is organized as follows. In the second section, the proposed PPIR algorithm is introduced, and the test schemes and results obtained on an FPGA platform are presented in Section 3. Discussion is given in Section 4. Finally, a conclusion is drawn in the last section.

2. PPIR Algorithm

Let us first assume that 2D circle labels are fixed on top of robots and the floor is flat. Estimated distances in lateral and longitudinal are discussed separately in the following subsections.

2.1. Estimation of Longitudinal Distance

A typical configuration of multiple robots in a formation and its perspective view on the TFT-LCD monitor is shown in **Fig. 2**, where label lengths for the leader and follower are respectively y_1 and y_0. They are separated by a distance d in longitudinal direction.

To find the real relative distance d by utilizing the perspective images with labels of the same dimension, the ratio between this distance and the label length can be ex-

pressed as:

$$\frac{d'}{y'_0} \leq \frac{d}{y_0} \leq \frac{d'}{y'_1}, \text{ and } y_0 = y_1 \quad \ldots\ldots\ldots (4)$$

where y'_0, y'_1 and d' represent respectively the relative perspective length of the follower, leader, and their relative distance on the flat monitor. Consequently, if both robots are very close to each other or the camera is perpendicularly oriented to the floor, the real distance may be roughly estimated by the average of the perspective label lengths:

$$\frac{d}{y_0} \cong \frac{1}{2}\left(\frac{d'}{y'_0} + \frac{d'}{y'_1}\right) = d'\left(\frac{y'_0 + y'_1}{2y'_0 y'_1}\right). \quad \ldots\ldots (5)$$

In real world operations, Eq. (5) will result in an intolerable error when the leader is moving further away, because the fast decreasing label length of the leader will be dominant, thus yielding a large positive error. Therefore, the ratio R_v denoted as d/y_0 can be estimated by its upper and lower limits as given in the following proposition.

Proposition 1: With a sufficiently small tilting angle, the ratio R_v is found between an upper limit, which is the average Perspective Projection Image Ratio (PPIR), and a lower limit as given in the following inequality:

$$d'\left(\frac{y'_0 + y'_1}{2y'_0 y'_1}\right) \cdot \delta_y \leq R_v \leq d'\left(\frac{y'_0 + y'_1}{2y'_0 y'_1}\right), \quad \ldots\ldots (6)$$

where $\delta_y = y'_1/y'_0$.

Proof:
To prove the relationship Eq. (6), one can translate the perspective image as:

$$y'_0 = ky_0, \quad y'_1 = \lambda y_0, \quad \ldots\ldots\ldots (7)$$

where $\lambda \leq k \leq 1$. So, with $y_0 = y_1$ and a small angle θ_0, due to similarity one can use the following trapezoidal formula:

$$d' \cong \frac{d(y'_0 + y'_1)}{y_0 + y_1} = \frac{R_v(\lambda y_0 + k y_0)}{2}, \quad \ldots\ldots (8)$$

where R_v denotes the ratio d/y_0. Now by substituting

$$\frac{d'}{y'_0} = \frac{R_v(\lambda + k)}{2k}, \quad \ldots\ldots\ldots (9)$$

and

$$\frac{d'}{y'_1} = \frac{R_v(\lambda + k)}{2\lambda}, \quad \ldots\ldots\ldots (10)$$

into Eq. (5) and noting $(\lambda + k)^2 \geq 4\lambda k$, one has

$$\frac{1}{2}\left(\frac{d'}{y'_0} + \frac{d'}{y'_1}\right) = \frac{R_v(\lambda + k)^2}{4k\lambda} \geq \frac{d}{y_0}. \quad \ldots\ldots (11)$$

This verifies the upper limit in Eq. (6). The lower limit can also be derived by noting $\lambda \leq k$:

$$\frac{R_v(\lambda + k)^2}{4k\lambda}\frac{\lambda y_0}{k y_0} = \frac{R_v(\lambda + k)^2}{4k^2} \leq \frac{d}{y_0}. \quad \ldots (12)$$

So the new estimated distance range can be rewritten as in Eq. (6).

The above proposition suggests the use of a coefficient δ_v which is greater than δ_y but less than 1 in order to estimate the real relative distance ratio in longitudinal direction as:

$$\frac{d}{y_0} = R_v \cong \frac{1}{2}\left(\frac{d'}{y'_0} + \frac{d'}{y'_1}\right) \cdot \delta_v, \quad \delta_y \leq \delta_v \leq 1 \quad \ldots (13)$$

To approximate δ_v in the proposed algorithm, we note the convergent series:

$$\sum_{i=1}^{\infty} \frac{1}{2^i} = 1, \quad \ldots\ldots\ldots\ldots\ldots (14)$$

which leads to the choice

$$\delta_v = \delta_y + \sum_{i=1}^{n} \frac{1}{2^i}(1 - \delta_y) = \frac{(2^n - 1)y'_0 + y'_1}{2^n y'_0}. \quad \ldots (15)$$

According to our experiments by using several generic digital cameras, the reasonable value for δ_v is obtained when n is between 3 and 4 for an expected tolerance less than 5% of the real distance.

Remark 1: By using Eq. (15) we can avoid the calculation of trigonometric functions in Eq. (3), and hence such algorithm as the CORDIC [20] is not used in our design.

Remark 2: It can be seen that coefficient δ_v can be adjusted automatically without requiring any additional optical installation or information of the camera. Particularly, in the case when both robots are found closely to each other or the camera has a zero tilt angle, the leader's label length y'_1 will converge to the label length of the follower, y'_0. This makes δ_v approach 1, and therefore Eq. (15) is simply brought to Eq. (5).

2.2. Estimation of Lateral Distance

In the lateral displacement of the robotic formation, shown in **Fig. 2**, the leader is moving parallelly to a follower on its left side. The label width of the leader, follower, and relative distance in real world coordinates are denoted as x_1, x_0, and s as shown in **Fig. 2(a)**, while the relative parameters of the perspective images are x'_1, x'_0, and s', as shown in **Fig. 2(b)**. In the lateral direction the relative distance may be estimated by using the above algorithm. However, due to the perspective phenomenon displaying on the TFT-LCD monitor, the oval image of the leader will be a little bit smaller than its follower (**Fig. 2(b)**). Correspondingly, coefficient δ_x can also be redefined as x'_1/x'_0. Now it follows that

$$s'\left(\frac{x'_0 + x'_1}{2x'_0 x'_1}\right) \cdot \delta_x \leq \frac{s}{x_0} \leq s'\left(\frac{x'_0 + x'_1}{2x'_0 x'_1}\right), \quad \ldots (16)$$

where

$$\frac{s}{x_0} = R_h \cong s'\left(\frac{x'_0 + x'_1}{2x'_0 x'_1}\right) \cdot \delta_h. \quad \ldots\ldots (17)$$

Finally, in light of Proposition 1 and by noting the $\delta_x \leq \delta_h \leq 1$, coefficient δ_h for the PPIR in the lateral direction is chosen as

$$\delta_h = \delta_x + \sum_{i=1}^{n} \frac{1}{2^i}(1-\delta_x) = \frac{(2^n-1)x_0' + x_1'}{2^n x_0'}. \quad . \quad (18)$$

2.3. Estimation of Euclidean Distance

Consider now the generic case of a triangular robotic formation, where the hypotenuse distance is obtained as:

$$R_s = \sqrt{R_v^2 + R_h^2}. \quad . \quad . \quad . \quad . \quad . \quad . \quad . \quad . \quad . \quad . \quad . \quad . \quad (19)$$

Remark 3: On the monitor screen, it may not be ready to determine the PPIR horizontal distance R_h of such a triangular formation due to the unavailability of the lateral label width with respect to the follower at the centreline. For reference, a virtual width x_t is adopted for x_0' in Eqs. (16)-(18) as:

$$x_t = \alpha x_0' = x_1', \quad . \quad . \quad . \quad . \quad . \quad . \quad . \quad . \quad . \quad . \quad . \quad . \quad (20)$$

where α is decided empirically such that the average error is less than 5% at any reasonable operational location in a half plane. This is illustrated in **Fig. 3** for deriving the relative distance in the lateral direction.

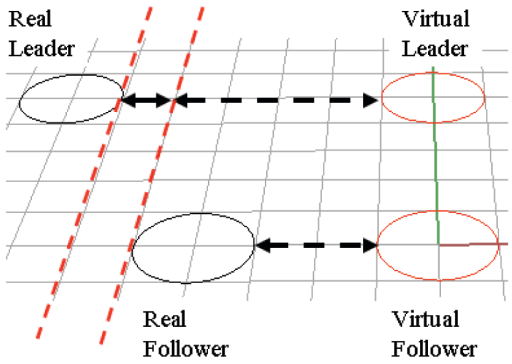

Fig. 3. Extended PPIR estimation in the lateral direction.

Table 1. PPIR test results with different degrees of n.

Tests	Real Distance (cm)	Error $n=3$ (%)	Error $n=4$ (%)
(a)	100	−3.37	+0.58
(b)	100	−2.3	+1.31
(c)	100	−3.17	+1.6
(d)	100	+4.7	+9.72
(e)	141.5	−1.7	+0.35

3. Experimental Results

3.1. Static Estimation

For the PPIR static estimation, the rigid circles (labels) are installed horizontally on top of miniature mobile robots, the Eyebots, having the same height. Circular discs are cut with 10 cm of diameter and the separation distance is set to 1 m edge to edge. The "blue" colour is chosen for the labels to improve the contrast. The general camera is used with 5M pixel resolution and adjustable focus from 7.1 to 21.4 mm. The focal length change is judged by reading the relative adjustable aperture range from f2.8 to f4.8. Constant α is set at 0.95.

To verify the estimation, the robots' perspective images are measured by a digital caliper. **Fig. 4** shows some of tested schemes with PPIR algorithm. From **Figs. 4(a)** to **(d)**, the images with the same longitudinal deployment are captured randomly by different tilted angles, installation heights, and focuses. In **Fig. 4(e)**, a basic triangular layout in the left plane is shown for simulating a formation scenario, where the robot located on the left-top corner represents the leading robot and the follower located at the bottom. The robot at the middle-top represents the virtual robot included here to account for the selection of constant α.

The estimation results about choosing the degree n for values of δ_v and δ_h in Eqs. (15) and (18) are demonstrated in the **Table 1**. When $n = 3$, the PPIR estimation has negative error while the positive error is observed with $n = 4$. The measured errors here are defined as the difference between the real value, 100 cm (141.5 cm), and the estimated distance in percentage.

Table 1 gave a summary to show the accuracy of PPIR in relative distance estimation. The value $n = 3$ yields less than 5% in error, which is quite satisfactory.

3.2. Dynamic Estimation

The devices used in the test scenarios are shown on **Fig. 5**. The Altera DE2-70 with Cyclone II FPGA is chosen as the FPGA development platforms used. For the miniature digital camera module, the Terasic TRDB-D5M is adopted with the maximum resolution for 5M pixels and fixed focal length. The frame rate of the camera is set for 34 fps with 1024×1280 pixels resolution.

Continuing our previous work on FPGA-based color discrimination [21], here we utilize a mobile robot carrying three bull-eye labels in a row formation. The leader is settled at the central position while followers are located at the both sides. One of the FPGA platforms is assigned to track the robots' labels by locating the blue circles in the inner area of labels. Meanwhile, another platform observes the relative ratio reading from the first FPGA platform. The blue circles are cut with a diameter of 6 cm, the arranged relative distance for any follower to the leader is 24 cm measuring from central points of the circular discs. Order n and α are chosen respectively as 3 and 0.95. Finally, results from both FPGA platforms are directly output to two TFT-LCD monitors via the VGA interface on the FPGA chips. The camera frame rates are shown on the 7-segment LED indicators as "22" reading in hexadecimal.

Figure 6 shows snapshots captured from the distance estimation video. The images presented on the left monitor screen show labels tracked from the ducking area while the measured relative distances are shown on the

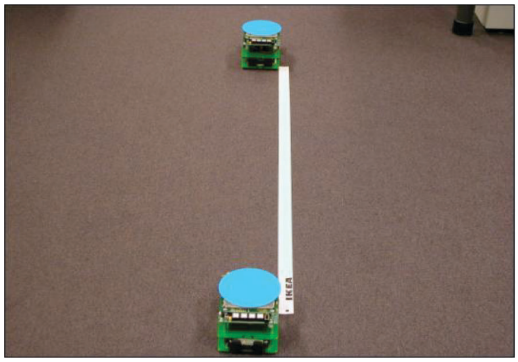

(a) Camera height: 111 cm/ tilted angle : 30°/ aperture: f4.0.

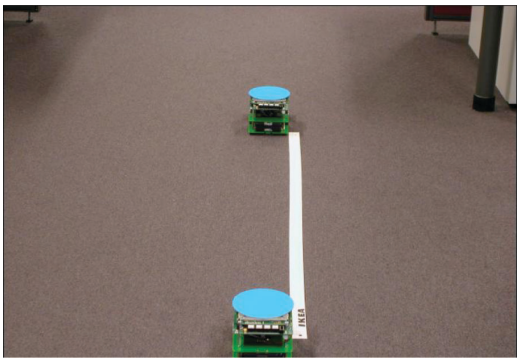

(b) Camera height: 111 cm/ tilted angle : 75°/ aperture: f4.8.

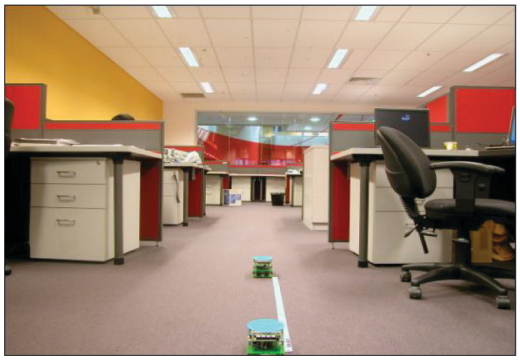

(c) Camera height: 51 cm/ tilted angle: 90°/ aperture: f2.8.

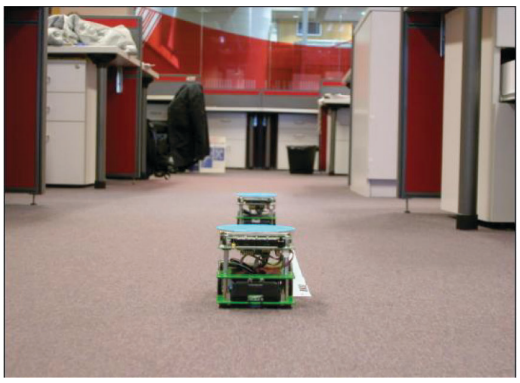

(d) Camera height: 19 cm/ tilted angle: 90°/ aperture: f4.0.

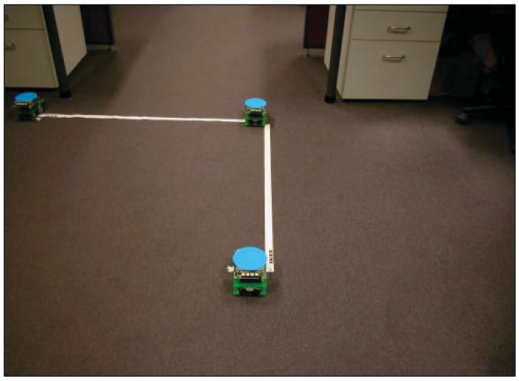

(e) Camera height: 112 cm/ tilted angle: 30°/ aperture: f2.9.

Fig. 4. Different scenarios in static testing.

right monitor screen, corresponding to the values at A and B positions. The reading are updated for every 0.5 second, and displayed by the ratio for 1 to 100, e.g., a distance of 4 (PPIR labels) is displayed as 400. The satisfactory accuracy of PPIR estimation can be verified from the results shown in **Figs. 6(a)**, **(b)**, and **(c)**.

All functions are implemented in hardware circuits for real-time processing taking into account the efficiency of logic gate usage. To achieve this, the floating point operations are not considered in our design. Here we suggest the floating number in PPIR algorithm to be re-scaled by simply multiplying 100 and keep the numbers in unsigned values for the basic binary operations, and the square root in Eq. (19) is executed by the abridged approximation [22]:

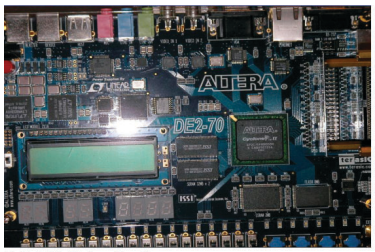

(a) FPGA platform.

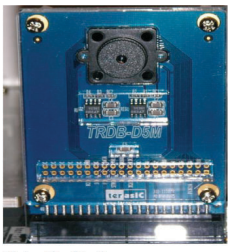

(b) digital camera

Fig. 5. FPGA platform and digital camera module.

$$\sqrt{R_v^2 + R_h^2} \cong \max\left(\left((a - 0.125a) + 0.5b\right), a\right), \quad . \quad (21)$$

where $a = \max(|R_v|, |R_h|)$, and $b = \min(|R_v|, |R_h|)$.

A simulated timing sequence of the PPIR algorithm be-

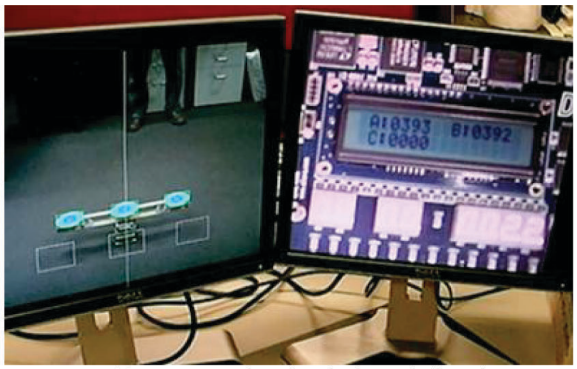

(a) PPIR estimation in lateral direction.

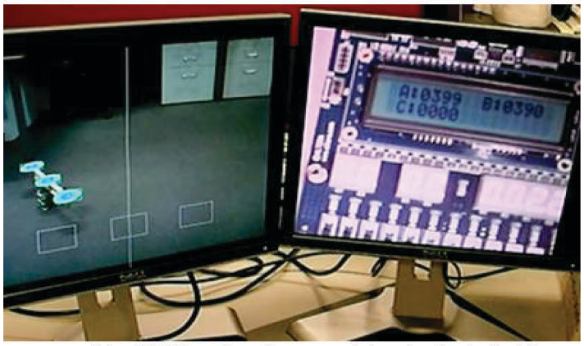

(b) PPIR estimation - cruising in the left side

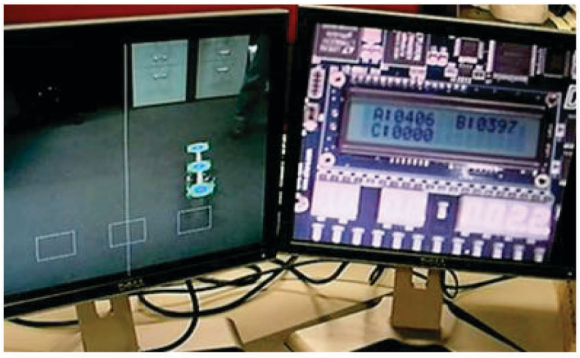

(c) The distance estimation - cruising in the right side

Fig. 6. PPIR estimation in dynamic testing.

tween two labels is shown in **Fig. 7**.

In implementation, the parallel processing circuit works with the camera pixel clock Pixel_clk of 77 MHz. The relative distance is calculated at the final line of the image sensor array, iYcont = 1023. The circular width and length labels expressed in pixels number are assigned as R_leader, L_leader, R_follower, L_follower, Up_leader, Down_leader, Up_follower, and Down_follower. The PPIR ratios in longitudinal and lateral directions are attained in 8 clocks (80 ns), see rRatio_v and rRatio_h, then the output results are obtained at oRatio_v and oRatio_h. The hypotenuse ratio by square rooting is performed only in 1 clock, shown in the last item "Distance."

The total resource usage of the FPGA platform is 30% of 68,416 logic elements in Cyclone II. That includes all

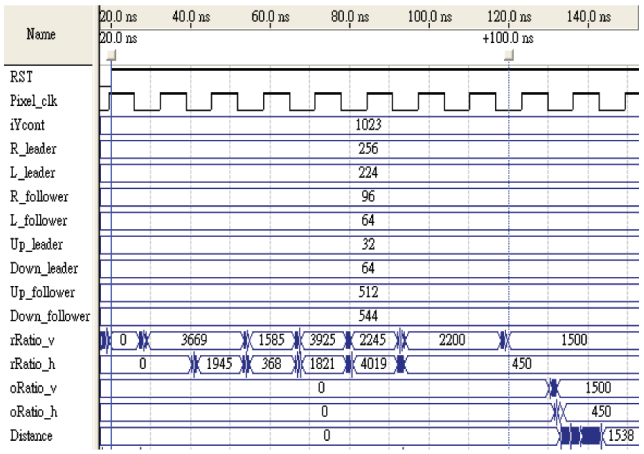

Fig. 7. Timing sequence of the PPIR algorithm.

image processing, labels tracking, VGA interface, test circuits for LCD displayer and 7-segment indicators, and the relative distance estimation for three robot labels.

4. Discussion

We have obtained satisfactory results in estimation of the relative distance between robots during static and dynamic test results with different cameras. It can be seen that the proposed algorithm can satisfactorily estimate the relative distance by using the perspective image changing ratio between robots. Moreover, the PPIR technique can track the real changing curve of the perspective distance without involving any complicated mathematical functions.

In reference to Eq. (3), computation time can be significantly reduced even without using a look-up table in memory, as in [19, 20]. Since a look-up table of CORDIC in external memory and floating point operations are not used in our design, resource usage can also be kept minimal, less than recursive computation.

Notably, the results obtained by using the proposed technique are not much affected by camera parameters. For example, within a reasonable working range, the PPIR algorithm is insensitive to the camera focal length. From **Fig. 4** and **Table 1**, it can be seen that the algorithm still maintains its accuracy even when the camera's focus is changed (variant aperture readings). Hence, the proposed technique can also be used with changing views with an adjustable focus for higher quality imaging.

The label designed as a circle leads to an elliptical shape in the perspective view for a better illustration of the derivation of the relative distances in both lateral and longitudinal directions. For different object sizes (robots), the dual circles in a concentric design may be used. After estimating the PPIR distance for the inner circle, the relative distance with larger dimensions of circles (robots) can be obtained by deducting the difference of radii from the PPIR distance.

5. Conclusion

In this paper we have proposed a new relative distance measurement algorithm for multi-robot systems with least calibration and computation efforts. With conventional distance measurement techniques, the low dynamic range of depth maps, complicated image algorithms, and high power consumption for active illumination may make the time-of-flight methodology unsuitable for compact indoor robot design. In contrast, the PPIR algorithm with a single digital camera is immune to these mentioned concerns. The algorithm is based on the upper and lower bounds of the perspective image ratio. By observing the labels attached to indoor mobile robots, the algorithm can calculate the relative distance accurately and instantly with different ratios between perspective labels and distance images. Simplicity in the algorithm derivation allows it to be implemented with the Field Programmable Gate Array (FPGA) technology. Experimental results demonstrate the effectiveness of the proposed technique.

References:

[1] N. Trawny, X. S. Zhou, K. X. Zhou, and S. I. Roumeliotis, "3D Relative Pose Estimation from Distance-Only Measurements," IEEE Int. Conf. on Intelligent Robots and Systems, San Diego, USA, pp. 1071-1078, 2007.

[2] M. K. Lee, J. O. Park, and J. E. S. Song, "User Authentication Based on Distance Estimation Using Ultrasonic Sensors," IEEE Int. Conf. Computation Intelligence and Security, Suzhou, China, pp. 391-394, 2008.

[3] C. Y. Wen, R. D. Morris, and W. A. Sethares, "Distance Estimation Using Bidirectional Communications Without Synchronous Clocking," IEEE Trans. on Signal Processing, Vol.55, No.5, pp. 1927-1939, 2007.

[4] W. Xiao, Y. Sun, Y. Liu, and Q. Yang, "TEA: Transmission Error Approximation for Distance Estimation between Two Zigbee Devices," IEEE Int. Conf. Networking, Architecture, and Storage, Shenyang, China, pp. 15-22, 2006.

[5] J. M. Dubois and H. Hüglí, "Time-of-flight imaging of indoor scenes with scattering compensation," Proc. of the 8th Conf. on Optical 3-D Measurement Techniques, Zurich, Switzerland, pp. 117-122, 2007.

[6] H. Rapp, "Experimental and Theoretical Investigation of Correlating TOF-Camera Systems," University of Heidelberg, pp. 59-63, Germany, 2007.

[7] J. H. Kim, "Ubiquitous Robot: Recent Progress and Development," Proc. IEEE/ SICE Int. Conf Digital Object Identifier, Busan, Korea, pp. 25- 30, 2006.

[8] Y. Y. Li, W. R. Fan, Y. R. Liu, and X. P. Cai, "Teleoperation of Robots via the Mobile Communication Networks," IEEE Int. Conf. Robotics and Biomimetics, Hong Kong, pp. 670-675, 2005.

[9] A. Stubbs, V. Vladimerou, A. T. Fulford, D. King, J. Strick, and G. E. Dullerud, "Multivehicle Systems Control over Networks: a hovercraft testbed for networked and decentralized control," IEEE Control System Magazine, Vol.26, No.3, pp. 56-69, 2006.

[10] Q. Chen, F. Tan, and P. Y. Woo, "An Improved Distance Measurement Method for Four-Legged Robots Based on the Colour Region," Proc. IEEE Int. Conf. on Intelligent Control and Automation, Chongqing, China, pp. 3040-3044, 2008.

[11] N. Yamaguti, S. Oe, and K. Terada, "A method of distance measurement by using monocular camera," Proc. 36th SICE Int. Conf., Tokushima, Japan, pp. 1255-1260, 1997.

[12] J. Chang and C. W. Cho, "Vision-Based Front Vehicle Detection and Its Distance Estimation," IEEE Int. Conf. on System, Man, and Cybernetics, Taipei, Taiwan, pp. 2063-2068, 2006.

[13] A. D. Nguyen, V. T. Ngo, Q. P. Ha, and G. Dissanayake, "Robotic Formation: Initialisation, Trajectory Planning, and Decentralised Control," Int. Journal of Automation and Control, Vol.2, No.1, pp. 22-45, 2008.

[14] R. D'Andrea and P. Wurman, "Future challenges of coordinating hundreds of autonomous vehicles in distribution facilities," IEEE Int. Conf. Technologies for Practical Robot Application, Woburn, USA, pp. 80-83, 2008.

[15] V. Vladimerou, A. Stubbs, J. Rubel, A. Fulford, J. Strick, and G. E. Dullerud, "A hovercraft testbed for decentralized and cooperative control," Proc. American Control Conf., Vol.6, pp. 5332-5337, 2004.

[16] R. Hartley and A. Zisserman, Multiple View Geometry in Computer Vision, Cambridge University Press, UK, pp. 153-236, 2003.

[17] M. Galer, "Digital Photography in Available Light," Elsevier, UK, pp. 224, 2006.

[18] Y.-H. Yu, N. M. Kwok, and Q. P. Ha, "FPGA-based Real-Time Color Tracking for Robotic Formation Control," Proc. Int. Conf. Robotics & Automation in Construction, Austin, USA, pp. 252-258, 2009.

[19] J. Kurian and P. R. S. Pillai, "A realization of an FPGA subsystem for reducing odometric localization errors in wheeled robots," J. of Automation, Mobile Robotics & Intelligent Systems, Vol.3, No.3, pp. 26-33, 2009.

[20] J.-P. Deschamps, G. J. A. Bioul, and G. D. Sutter, "Synthesis of Arithmetic Circuits," John Wiley & Sons, Canada, 2006.

[21] Y.-H. Yu, Q. P. Ha, and N. M. Kwok, "FPGA-based Real-time Color Discrimination Design for Ubiquitous Robots," Proc. Australasian Conf. on Robotics and Automation, Sydney, Australia, 2009.

[22] P. P. Chu, "RTL Hardware Design Using VHDL," John Wiley & Sons, Canada, pp. 460-468, 2006.

Name:
Ying-Hao Yu

Affiliation:
Ph.D. Candidate, Faculty of Engineering and Information Technology, University of Technology Sydney (UTS)

Address:
PO Box 123, Broadway NSW 2007, Australia

Brief Biographical History:
2005 Obtained his Masters in Information Technology from The University of Newcastle Australia

Main Works:
• FPGA based Ubiquitous intelligence, multi-robot formation driving control

Name:
Chau Vo-Ky

Affiliation:
Faculty of Electrical and Electronics Engineering, HoChiMinh City University of Technology

Address:
268 Ly Thuong Kiet St., Distr. 10, HoChiMinh City, Vietnam

Brief Biographical History:
2003 Obtained his MEng in Electronics & Telecommunication Engineering from HoChiMinh City University of Technology, Vietnam

Main Works:
• control, communication systems, System-on-Chip and embedded system applications

Name:
Sarath Kodagoda

Affiliation:
Faculty of Engineering and Information Technology, University of Technology Sydney (UTS)

Address:
PO Box 123, Broadway NSW 2007, Australia

Brief Biographical History:
2004 Ph.D. in the field of robotics from Nanyang Technological University, Singapore
2008- Senior Lecturer at Faculty of Engineering and Information Technology, UTS, Australia

Main Works:
• robotics, data fusion, human robot interaction, intelligent transportation systems and road safety

Membership in Academic Societies:
• Member, the Institution of Engineering and Technology (IET)

Name:
Quang Phuc Ha

Affiliation:
Faculty of Engineering and Information Technology, University of Technology Sydney (UTS)

Address:
PO Box 123, Broadway NSW 2007, Australia

Brief Biographical History:
1993 Obtained his Ph.D. in Electrical Engineering from Moscow Power Engineering Institute, Russia
2006- Associate Professor at Faculty of Engineering and Information Technology, UTS, Australia

Main Works:
• control and automation, robotics, and computational intelligence applications.

Membership in Academic Societies:
• Member, Institute of Electrical and Electronics Engineers, Inc. (IEEE)
• Board of Directors, The International Association of Automation and Robotics in Construction (IAARC)
• Associate Editor, The IEEE Transactions on Automation Science and Engineering
• Editorial Board, The International Journal of Automation and Control
• Associate Editor, The Journal of Advanced Computational Intelligence and Intelligent Informatics